A DIRECT MEASUREMENT OF THE HEAT RELEASE IN THE OUTER CRUST OF THE TRANSIENTLY ACCRETING NEUTRON STAR XTE J1709−267

N. Degenaar[1,3], R. Wijnands[2], AND J. M. Miller[1]
[1] Department of Astronomy, University of Michigan, 500 Church Street, Ann Arbor, MI 48109, USA; degenaar@umich.edu
[2] Astronomical Institute Anton Pannekoek, University of Amsterdam, Postbus 94249, 1090 GE Amsterdam, The Netherlands
Received 2012 December 5; accepted 2013 March 20; published 2013 April 4

ABSTRACT

The heating and cooling of transiently accreting neutron stars provides a powerful probe of the structure and composition of their crust. Observations of superbursts and cooling of accretion-heated neutron stars require more heat release than is accounted for in current models. Obtaining firm constraints on the depth and magnitude of this extra heat is challenging and therefore its origin remains uncertain. We report on *Swift* and *XMM-Newton* observations of the transient neutron star low-mass X-ray binary XTE J1709−267, which were made in 2012 September–October when it transitioned to quiescence after a $\simeq$10 week long accretion outburst. The source is detected with *XMM-Newton* at a 0.5–10 keV luminosity of $L_X \simeq 2 \times 10^{34}(D/8.5\,\mathrm{kpc})^2$ erg s^{-1}. The X-ray spectrum consists of a thermal component that fits to a neutron star atmosphere model and a non-thermal emission tail, each of which contribute $\simeq$50% to the total flux. The neutron star temperature decreases from $\simeq$158 to $\simeq$152 eV during the $\simeq$8 hr long observation. This can be interpreted as cooling of a crustal layer located at a column density of $y \simeq 5 \times 10^{12}$ g cm^{-2} ($\simeq$50 m inside the neutron star), which is just below the ignition depth of superbursts. The required heat generation in the layers on top would be $\simeq$0.06–0.13 MeV per accreted nucleon. The magnitude and depth rule out electron captures and nuclear fusion reactions as the heat source, but it may be accounted for by chemical separation of light and heavy nuclei. Low-level accretion offers an alternative explanation for the observed variability.

Key words: accretion, accretion disks – dense matter – stars: neutron – X-rays: binaries – X-rays: individual (XTE J1709−267)

Online-only material: color figure

1. INTRODUCTION

Many observable properties of neutron stars are set by the structure and composition of their crust. Low-mass X-ray binaries (LMXBs) offer powerful means to investigate the properties of these layers. In LMXBs, a neutron star accretes matter from a late-type companion star that overflows its Roche lobe. This typically generates a 2–10 keV luminosity of $L_X \simeq 10^{35-38}$ erg s^{-1}. Transient LMXBs only occasionally experience outbursts of accretion, while they spend the majority of their time in a quiescent phase with little or no matter being accreted onto the neutron star. The quiescent X-ray emission is therefore much dimmer; $L_X \simeq 10^{31-34}$ erg s^{-1}.

Matter that falls onto the surface of a neutron star is compressed to higher densities as it becomes buried by freshly accreted material. As a result, the matter undergoes compositional changes that are driven by nuclear reactions. These involve thermonuclear burning near the stellar surface, electron captures and neutron emissions that occur a few tens of meters inside the neutron star, and nuclear fusion reactions that take place at several hundred meters depth (Sato 1979; Wallace & Woosley 1981; Haensel & Zdunik 1990; Schatz et al. 2001).

Initial calculations suggested that this chain of nuclear processes deposits an energy of $\simeq$1–1.5 MeV per accreted nucleon in the neutron star crust (Haensel & Zdunik 1990, 2003). However, observations of superbursts and the thermal evolution of neutron stars after an accretion phase both require a hotter crust than these heating rates account for (Cumming et al. 2006; Brown & Cumming 2009; Degenaar et al. 2011a). The discrepancy may be resolved if there is an additional source of heat from nuclear reactions or other processes in the outer crustal layers (Gupta et al. 2007; Horowitz et al. 2008; Medin & Cumming 2011).

During outburst, the energy that is generated in the crust creates a temperature profile that depends on the depth and magnitude of the heat sources. During quiescence, the gained heat is thermally conducted toward the surface and the core, until the crust has cooled and thermal equilibrium is restored. The cooling of neutron star crusts can be observed as a decrease in quiescent thermal X-ray emission after the end of an accretion outburst (Wijnands et al. 2002, 2004; Cackett et al. 2008, 2010a; Degenaar et al. 2009, 2011a, 2011b; Díaz Trigo et al. 2011; Fridriksson et al. 2010, 2011).

Comparing crust cooling observations with neutron star thermal evolution models yields important insight into the properties of the crust and core (Rutledge et al. 2002b; Shternin et al. 2007; Brown & Cumming 2009; Degenaar et al. 2011a; Page & Reddy 2012). However, the current data provide only weak constraints on any additional heat sources. Progress can be made by observing the temperature evolution shortly (within $\simeq$2 weeks) after the end of an outburst, since that can provide a direct measure of the depth and magnitude of the heat release in the outer crust (Brown & Cumming 2009; Degenaar et al. 2011a).

XTE J1709−267 (1RXS J170930.2−263927) is a neutron star LMXB that was first reported in outburst in 1997 (Marshall et al. 1997). The source is thought to be associated with the globular cluster NGC 6293 (Jonker et al. 2004b), which would place it at a distance of $\simeq$8.5 kpc (Harris 1996; Lee & Carney 2006). In the past 15 years, it has exhibited several
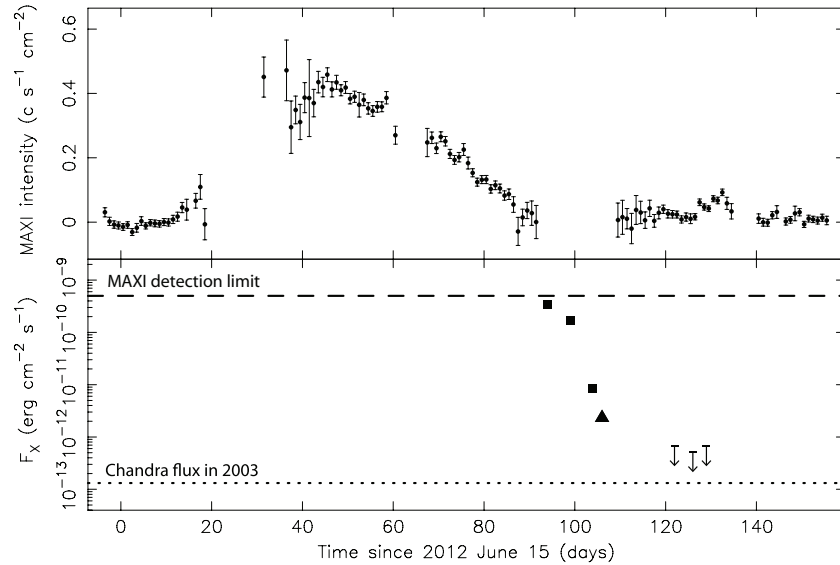
---

[3] Hubble fellow.

Figure 1. Top: one day averaged *MAXI* light curve of the 2012 outburst (2–20 keV). Bottom: evolution of the unabsorbed 0.5–10 keV flux after the source intensity dropped below the detection limit of *MAXI* (dashed line). The squares and upper limits represent *Swift* data, and the triangle indicates the *XMM-Newton* observation. The dotted line corresponds to the flux measured with *Chandra* in 2003.

Table 1
X-Ray Observation Log

Observatory	Date	Obs ID	Exposure Time (ks)
Swift	2012 Sep 18	35717011	0.9
Swift	2012 Sep 23	35717012	0.8
Swift	2012 Sep 28	35717013	0.9
XMM-Newton	2012 Sep 30	0700381401	31
Swift	2012 Oct 16	35717014	0.9
Swift	2012 Oct 20	35717015	1.1
Swift	2012 Oct 23	35717016	0.9

Note. After excluding a short episode of background flaring, the net exposure time of the *XMM-Newton* observation was $\simeq$30 ks for the PN and $\simeq$28 ks for the MOS1.

accretion outbursts with a typical 2–10 keV intensity of $L_X \simeq 2 \times 10^{37}(D/8.5\,\mathrm{kpc})^2\,\mathrm{erg\,s}^{-1}$ (Marshall et al. 1997; Cocchi et al. 1998; Jonker et al. 2003, 2004a, 2004b; Markwardt & Swank 2004; Remillard 2007; Negoro et al. 2010; Yamauchi 2010).

The most recent outburst occurred in 2012 June–September (Sanchez-Fernandez et al. 2012). Figure 1 displays the light curve as observed with *MAXI*. The source was active for $\simeq$10 weeks with an average 2–10 keV flux of $F_X \simeq 2 \times 10^{-9}\,\mathrm{erg\,cm}^{-2}\,\mathrm{s}^{-1}$. Its intensity remained below the detection limit of *MAXI* from September 11 onward, marking its return to quiescence (Figure 1).

In this work we report on a series of *Swift* pointings and an *XMM-Newton* observation of XTE J1709−267. The data were obtained in 2012 September–October, and aimed to search for signs of an accretion-heated crust.

2. OBSERVATIONS, DATA ANALYSIS, AND RESULTS

The observations discussed in this work are listed in Table 1. All spectral data were fitted between 0.5 and 10 keV using XSPEC (version 12.7; Arnaud 1996). Interstellar absorption was taken into account by using the TBABS model (Wilms et al. 2000). Throughout this work we assumed a source distance of $D = 8.5$ kpc. All quoted errors refer to 1σ confidence intervals.

2.1. Swift

XTE J1709−267 was observed with *Swift* six times (Table 1). Data reduction and analysis was carried out within HEASOFT (version 6.11). We re-processed the raw data obtained with the X-ray Telescope (XRT) using the XRTPIPELINE. Spectra and light curves were extracted using XSELECT.

The first two XRT observations were affected by pile-up. We therefore extracted source events using an annular region with inner and outer radii of $12''$ and $60''$ for observation 35717011, and $10''$ and $60''$ for 35717012. For the other four observations we used a circular region with a radius of $15''$. Background events were collected from a source-free circular region with a radius of $45''$.

2.1.1. X-ray Spectra and Light Curve

The first series of *Swift* observations were obtained on September 18, 23, and 28. We fitted the XRT spectra of these three data sets simultaneously to a simple absorbed power-law model. This resulted in a joint value of $N_H = (3.4 \pm 0.3) \times 10^{21}\,\mathrm{cm}^{-2}$ and power-law indices of $\Gamma = 2.0 \pm 0.1$, 2.4 ± 0.1, and 2.6 ± 0.3 for the first, second, and third observation, respectively (yielding $\chi^2_\nu = 0.93$ for 118 dof). The corresponding unabsorbed 0.5–10 keV fluxes are $F_X = (3.4 \pm 0.2) \times 10^{-10}$, $(1.7 \pm 0.2) \times 10^{-10}$, and $(8.4 \pm 1.3) \times 10^{-12}\,\mathrm{erg\,cm}^{-2}\,\mathrm{s}^{-1}$ (Figure 1).

The intensity and spectral shape suggest that the source was still in outburst during the first two *Swift* observations, but that accretion may have ceased by the time of the third. We therefore attempted to fit this spectrum with the model inferred from the *XMM-Newton* data (Section 2.2.1). Leaving only the neutron star temperature and power-law normalization as free fit parameters results in $kT^\infty \gtrsim 191$ eV. This is not unphysical and may indicate that the neutron star surface was visible.

The second series of *Swift* pointings were performed on October 16, 20, and 23. XTE J1709−267 is not detected in these observations. We determined 95% upper limits on the count rate by applying the prescription for small numbers of counts given by Gehrels (1986). Corresponding upper limits on the 0.5–10 keV unabsorbed flux were estimated using

PIMMS (version 4.6) by assuming a power-law spectrum with $N_H = 4.9 \times 10^{21}$ cm^{-2} and $\Gamma = 2.9$ (see Section 2.2.1). This yielded $F_X \lesssim (3-7) \times 10^{-13}$ erg cm^{-2} s^{-1}. Summing the three observations reveals a small excess of photons at the source position for which we estimate $F_X \simeq 2 \times 10^{-13}$ erg cm^{-2} s^{-1}. This is a factor of $\simeq 2$ higher than the quiescent level observed with *Chandra* in 2002 (see Section 2.2.1). Figure 1 displays the flux light curve of the *Swift* observations.

2.2. XMM-Newton

XMM-Newton observed XTE J1709$-$267 for 31 ks starting on UT 2012 September 30 at 09:47. We analyzed the data obtained with the European Photon Imaging Camera (EPIC). The PN and the MOS1 were both set in small window imaging mode. The source was not detected with the MOS2, which was operated in timing mode. Data reduction and analysis was carried out using the Science Analysis Software (SAS; version 11.0.0).

A short episode of background flaring was excluded by selecting data with high-energy count rates of <0.15 counts s^{-1} for the PN (10–12 keV) and <0.30 counts s^{-1} for the MOS1 (>10 keV). This resulted in a total net exposure time of $\simeq 30$ and $\simeq 28$ ks for the PN and the MOS1, respectively. We extracted source events from a circular region with a radius of 30″, and used a source-free circular region with a radius of 60″ for the background.

XTE J1709$-$267 is detected at an average net count rate of 0.568 ± 0.006 counts s^{-1} with the PN and at 0.195 ± 0.003 counts s^{-1} with the MOS1. Background-corrected light curves were created using the tasks EVSELECT and LCCORR. The X-ray spectra and response files were extracted using the task ESPECGET. The spectral data were grouped to contain >20 photons per bin.

2.2.1. Average X-ray Spectrum

We fitted the PN and MOS1 spectral data simultaneously with all parameters tied between the two instruments. A simple absorbed power-law model (PEGPWRLW) yields $N_H = (4.9 \pm 0.1) \times 10^{21}$ cm^{-2} and $\Gamma = 2.90 \pm 0.04$ ($\chi_\nu^2 = 1.32$ for 506 dof). The fit can be significantly improved by adding a thermal component. We used the neutron star atmosphere model NSATMOS (Heinke et al. 2007). In all fits we fixed the mass and radius to canonical values of $M = 1.4 M_\odot$ and $R = 10$ km, adopted a distance of $D = 8.5$ kpc, and set the normalization constant at 1 (i.e., the entire surface is radiating). This left the neutron star temperature as the only free fit parameter.

The composite model provides a good fit, yielding $N_H = (2.9 \pm 0.1) \times 10^{21}$ cm^{-2}, $\Gamma = 1.34 \pm 0.11$, and $kT^\infty = 155.7 \pm 1.4$ eV ($\chi_\nu^2 = 1.04$ for 505 dof). The spectral data and model fit are shown in Figure 2. The inferred 0.5–10 keV unabsorbed flux is $F_X = (2.33 \pm 0.01) \times 10^{-12}$ erg cm^{-2} s^{-1}, which translates into a luminosity of $L_X = (2.01 \pm 0.01) \times 10^{34}(D/8.5\,\text{kpc})^2$ erg s^{-1}. The power-law component contributes $46\% \pm 2\%$ to the total unabsorbed flux. By setting the power-law normalization to zero and extrapolating the NSATMOS model fit to the 0.01–100 keV range, we estimate a thermal bolometric flux of $F_{bol} = (1.5 \pm 0.1) \times 10^{-12}$ erg cm^{-2} s^{-1}.

We compare these results with the quiescent properties measured with *Chandra* on 2003 May 12 (Obs ID 3507; for details, see Jonker et al. 2004b). We reduced the data using the CIAO tools (version 4.4) and extracted a background-corrected spectrum. We fitted this with a combined power law and neutron star atmosphere model, with $N_H = 2.9 \times 10^{21}$ cm^{-2} and $\Gamma = 1.3$ fixed to the values inferred from the *XMM-Newton*
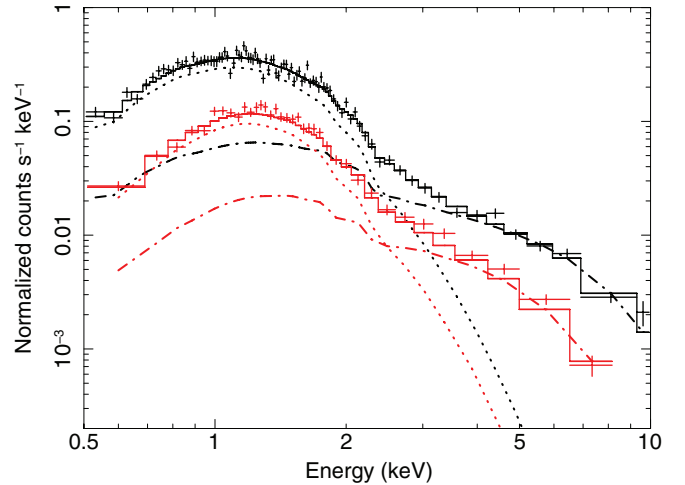

Figure 2. PN (top, black) and MOS1 (bottom, red) spectra. The solid line represents the best fit to a combined neutron star atmosphere (dotted lines) and power-law (dashed-dotted curves) model. The spectra were rebinned for representation purposes.

(A color version of this figure is available in the online journal.)

data. This yielded $kT^\infty = 88.6 \pm 8.7$ eV and a 0.5–10 keV unabsorbed flux of $F_X = (1.32 \pm 0.09) \times 10^{-13}$ erg cm^{-2} s^{-1}, of which $25\% \pm 10\%$ can be attributed to the power-law emission ($\chi_\nu^2 = 0.84$ for 14 dof).

2.2.2. A Decay in X-Ray Flux

The PN and MOS1 light curves reveal that the intensity of XTE J1709$-$267 decreased during the observation. The co-added light curve is shown in Figure 3. To investigate the cause of this decay, we divided the data into three equal parts of $\simeq 10$ ks and analyzed the individual spectra. We used the combined power law and neutron star atmosphere model described in Section 2.2.1 and required the hydrogen column density to be the same between the three data segments (for a justification, see Miller et al. 2009).

The results of the time-resolved spectroscopy are shown in Figure 4. This suggests that the flux of both the thermal and the power-law component decreased during the observation. The fractional contribution of the power law to the total unabsorbed 0.5–10 keV flux was consistent with being constant: $48\% \pm 3\%$, $46\% \pm 3\%$, and $45\% \pm 3\%$ for the first, second, and third intervals, respectively. The neutron star temperature decreased $\simeq 2.5\sigma$ during the observation, from $kT^\infty = 158.4 \pm 2.5$ to 152.0 ± 2.1 eV. The power-law index remained constant within the errors (Figure 4).

3. DISCUSSION

We report on *Swift* and *XMM-Newton* observations obtained during the decay of the 2012 outburst of XTE J1709$-$267. The data cover a time span of 35 days, during which the source intensity decreases from $L_X \simeq 3 \times 10^{36}$ to $\simeq 2 \times 10^{33}(D/8.5\,\text{kpc})^2$ erg s^{-1} (0.5–10 keV).

The spectral data can be described by an absorbed power law that softens from $\Gamma = 2.0$ to 2.6 in the first set of *Swift* observations, and further to $\Gamma = 2.9$ when fitting the *XMM-Newton* data with the same model. Similar softening has been observed in other transient LMXBs for which high-quality spectral data were obtained during the transition from outburst
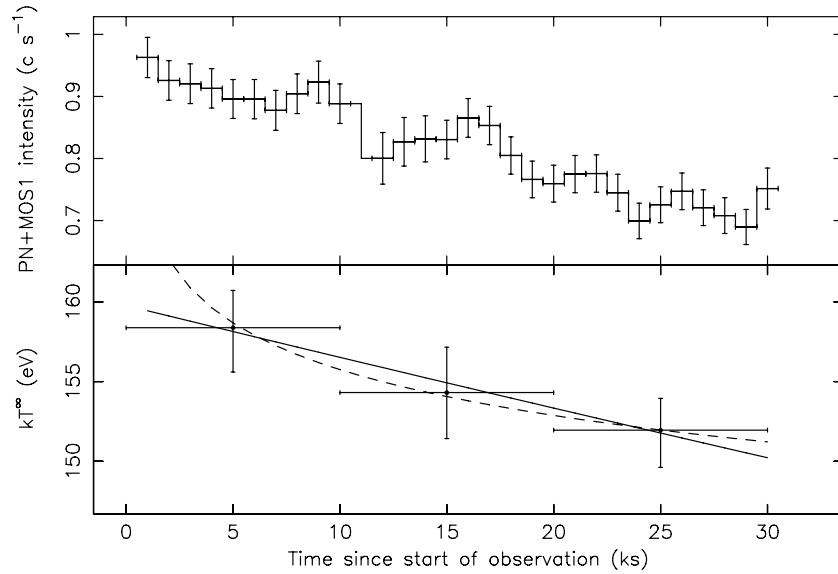
Figure 3. Top: combined PN/MOS1 light curve using a bin time of 1000 s. Bottom: evolution in neutron star temperature along with a fit to a power-law decay with an index of −0.03 (dashed curve) and an exponential decay of 5.6 days (solid line).
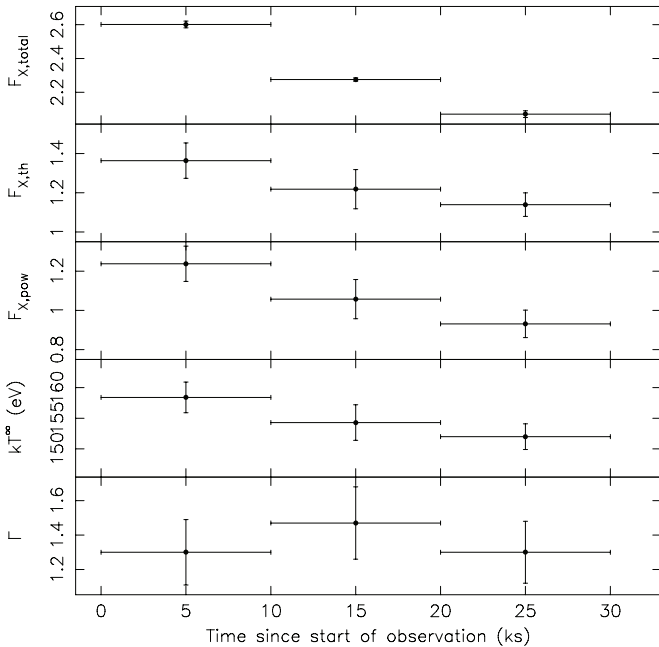

Figure 4. Results of time-resolved spectroscopy of the PN and MOS1 data. From top to bottom: the total unabsorbed model flux, thermal flux, and power-law flux (0.5–10 keV and units of 10^{-12} erg cm^{-2} s^{-1}), the neutron star temperature, and the power-law index.

to quiescence (for an in depth discussion, see Armas Padilla et al. 2011, 2013). The *XMM-Newton* data of XTE J1709−267 are much better described by adding a thermal component, which suggests that at least part of the observed softening is not caused by the power-law emission itself, but by a soft component becoming apparent in the spectrum.

XTE J1709−267 is detected with *XMM-Newton* at a 0.5–10 keV luminosity of $L_X \simeq 2 \times 10^{34}(D/8.5 \text{ kpc})^2$ erg s^{-1}. The spectral data are best fit with a composite model consisting of a thermal emission component that can be described by a neutron star atmosphere with a temperature of $kT^{\infty} \simeq 156$ eV, and a non-thermal emission tail that fits to a power law with an

index of $\Gamma \simeq 1.3$ and contributes $\simeq 50\%$ to the total unabsorbed 0.5–10 keV flux. Such a spectral shape is common for neutron star LMXBs in quiescence.

The 0.5–10 keV flux measured during the *XMM-Newton* observation is a factor $\simeq 20$ higher than seen with *Chandra* in 2003 ($\simeq 1$ year after the end of its 2002 outburst), and the inferred neutron star temperature is higher by a factor of $\simeq 1.7$. The subsequent *Swift* observations show that the thermal emission had decreased, but was still a factor of $\simeq 2$ above the level detected with *Chandra*. This may indicate that (part of) the crust became substantially heated during the recent $\simeq 10$ week outburst, and was cooling in quiescence.

Most remarkably, we found that the intensity of XTE J1709−267 decreased during the $\simeq 8$ hr long *XMM-Newton* observation. Time-resolved spectroscopy suggests that the neutron star temperature decreased from $\simeq 158$ to $\simeq 152$ eV. An attractive explanation is that the outburst indeed heated the crust and that it was cooling during our observation (see Section 3.1). However, the presence of a strong and variable non-thermal emission component suggests that residual accretion was possibly occurring.

Multi-epoch studies of a number of neutron stars LMXBs have shown (non-monotonic) variations in the quiescent thermal emission that cannot be attributed to cooling of a heated crust (Rutledge et al. 2002a; Campana et al. 2004; Cackett et al. 2010b; Fridriksson et al. 2010). Correlated variability with the power-law component suggests that a residual accretion flow may reach the neutron star in some sources (Cackett et al. 2010b; Fridriksson et al. 2010). This would generate a thermal spectrum that is difficult to distinguish from that of a cooling neutron star (Zampieri et al. 1995; Soria et al. 2011). In this case the inferred temperature does not reflect that of the neutron star crust, but rather that of the surface that continues to be heated by the ongoing accretion.

Time-resolved spectroscopy indicates that the thermal and the power-law component may both have varied during the *XMM-Newton* observation of XTE J1709−267. This suggests that matter was possibly still being accreted onto the neutron star. An alternative explanation is therefore that the observed flux decrease was caused by variations in the accretion rate.

4

3.1. Constraining the Heat Release in the Outer Crust

If the decrease in temperature observed during our *XMM-Newton* observation was due to cooling of the neutron star crust, then we can use this result to constrain the heat release in the crust. At any given depth inside the neutron star, it takes a certain characteristic time for heat to diffuse to the surface, i.e., for the layer to cool. The observed decrease in neutron star temperature from $kT^\infty \simeq 158$ to $\simeq 152$ eV can be fitted with an exponential decay time of $\simeq 5.6 \pm 1.9$ days (Figure 3). Using Equation (9) of Brown & Cumming (2009), we find that this is the characteristic cooling time for a layer located at a column depth of $y \simeq 5 \times 10^{12}$ g cm^{-2} (corresponding to a matter density of $\rho \simeq 2 \times 10^9$ g cm^{-3}, or a depth of $\simeq 50$ m inside the neutron star). This is just below the depth where superbursts are thought to ignite (Cumming et al. 2006).

The decrease in temperature can also be described by a power-law decay with a slope of -0.03 ± 0.01 (Figure 3). This can be used to estimate the heat flux in the crust; using Equations (8)–(11) of Brown & Cumming (2009), we find $F_{crust} = (1.0–2.0) \times 10^{21}$ erg cm^{-2} s^{-1}. Combining this with the mass-accretion rate provides an estimate of the energy that was released in the crust during outburst.

The average intensity observed with *MAXI* during the 2012 outburst translates into a 2–10 keV luminosity of $L_X \simeq 2 \times 10^{37}(D/8.5\,\mathrm{kpc})^2$ erg s^{-1}. The bolometric luminosity of neutron star LMXBs is typically a factor of $\simeq 2.5$ higher than measured in the 2–10 keV band (in 't Zand et al. 2007), which would imply an average accretion luminosity of $L_{acc} \simeq 4 \times 10^{37}(D/8.5\,\mathrm{kpc})^2$ erg s^{-1}. This gives an estimated mass-accretion rate of $\dot{M}_{ob} = RL_{acc}/GM \simeq 2.1 \times 10^{17}$ g s^{-1} (for $R = 10$ km and $M = 1.4\,M_\odot$). Assuming that the emission is isotropic, the mass-accretion rate per surface area is $\dot{m}_{ob} \simeq 1.7 \times 10^4$ g cm^{-2} s^{-1}. We then find a heat release of $F_{crust}/\dot{m}_{ob} \simeq (6–12) \times 10^{16}$ erg g$^{-1} \simeq 0.06–0.13$ MeV per accreted nucleon. This heat must have been produced in the layers above the cooling layer that is probed by our observation, i.e., at a depth of $y \lesssim 5 \times 10^{12}$ g cm^{-2}.

We can compare these constraints with the different mechanisms that have been put forward as possible sources of extra heat release in the neutron star crust. The shallow depth ($y \lesssim 5 \times 10^{12}$ g cm^{-2}) rules out nuclear fusion reactions, since these occur much deeper in the crust ($y \gtrsim 10^{14}$ g cm^{-2}; Horowitz et al. 2008). Electron captures do occur at the inferred depth, but these are expected to generate a heat of $\simeq 0.01$ MeV nucleon^{-1} (Gupta et al. 2007; Estradé et al. 2011), which is a factor of $\simeq 10$ lower than we obtain.

Chemical separation in the crust provides an alternative mechanism for the heat release. Just below the surface, the crust is composed of a variety of ions that effectively behave as a liquid. This is commonly referred to as the neutron star "ocean" and is thought to be the ignition site of superbursts. The matter freezes out at the bottom of the ocean, at $y \simeq 10^{12}$ g cm^{-2}, becoming part of the solid crust. Molecular dynamics simulations suggest that the freezing of a mixture of elements causes chemical separation, with light nuclei mainly being left in the liquid phase and heavier nuclei preferentially becoming incorporated in the solid crust (Horowitz et al. 2007). The retention of light elements in the liquid ocean drives a buoyancy that can cause a convective heat flux of $\simeq 0.01–0.2$ MeV per accreted nucleon, depending on the composition (Medin & Cumming 2011).

We conclude that within our current knowledge, electron captures and nuclear fusion reactions cannot be the source of

shallow heat that may be present in XTE J1709−267. Instead, chemical separation of light and heavy nuclei can account for both the depth and the magnitude of the heat source that we infer from our *XMM-Newton* observation. If cooling of a crustal layer is causing the observed flux decrease, this suggests that chemical separation may play an important role in heating the crusts of neutron stars. This process can then potentially supply the extra heat that is required to resolve the discrepancy between current heating models, observations of superbursts, and crust cooling of accretion-heated neutron stars.

REFERENCES

Armas Padilla, M., Degenaar, N., Patruno, A., et al. 2011, MNRAS, 417, 659
Armas Padilla, M., Degenaar, N., Russell, D. M., & Wijnands, R. 2013, MNRAS, 428, 3083
Arnaud, K. A. 1996, in ASP Conf. Ser. 101, Astronomical Data Analysis Software and Systems V, ed. G. H. Jacoby & J. Barnes (San Francisco, CA: ASP), 17
Brown, E. F., & Cumming, A. 2009, ApJ, 698, 1020
Cackett, E. M., Brown, E. F., Cumming, A., et al. 2010a, ApJL, 722, L137
Cackett, E. M., Brown, E. F., Miller, J. M., & Wijnands, R. 2010b, ApJ, 720, 1325
Cackett, E. M., Wijnands, R., Miller, J. M., Brown, E. F., & Degenaar, N. 2008, ApJL, 687, L87
Campana, S., Israel, G. L., Stella, L., Gastaldello, F., & Mereghetti, S. 2004, ApJ, 601, 474
Cocchi, M., Bazzano, A., Natalucci, L., et al. 1998, ApJL, 508, L163
Cumming, A., Macbeth, J., in 't Zand, J. J. M., & Page, D. 2006, ApJ, 646, 429
Degenaar, N., Brown, E. F., & Wijnands, R. 2011a, MNRAS, 418, L152
Degenaar, N., Wijnands, R., Wolff, M. T., et al. 2009, MNRAS, 396, L26
Degenaar, N., Wolff, M. T., Ray, P. S., et al. 2011b, MNRAS, 412, 1409
Díaz Trigo, M., Boirin, L., Costantini, E., Méndez, M., & Parmar, A. 2011, A&A, 528, 150
Estradé, A., Matoš, M., Schatz, H., et al. 2011, PhRvL, 107, 172503
Fridriksson, J. K., Homan, J., Wijnands, R., et al. 2010, ApJ, 714, 270
Fridriksson, J. K., Homan, J., Wijnands, R., et al. 2011, ApJ, 736, 162
Gehrels, N. 1986, ApJ, 303, 336
Gupta, S., Brown, E. F., Schatz, H., Möller, P., & Kratz, K.-L. 2007, ApJ, 662, 1188
Haensel, P., & Zdunik, J. L. 1990, A&A, 227, 431
Haensel, P., & Zdunik, J. L. 2003, A&A, 404, L33
Harris, W. E. 1996, AJ, 112, 1487
Heinke, C. O., Jonker, P. G., Wijnands, R., & Taam, R. E. 2007, ApJ, 660, 1424
Horowitz, C. J., Berry, D. K., & Brown, E. F. 2007, PhRvE, 75, 066101
Horowitz, C. J., Dussan, H., & Berry, D. K. 2008, PhRvC, 77, 045807
in 't Zand, J. J. M., Jonker, P. G., & Markwardt, C. B. 2007, A&A, 465, 953
Jonker, P. G., Buxton, M., & McClintock, J. E. 2004a, ATel, 262, 1
Jonker, P. G., Galloway, D. K., McClintock, J. E., et al. 2004b, MNRAS, 354, 666
Jonker, P. G., Méndez, M., Nelemans, G., Wijnands, R., & van der Klis, M. 2003, MNRAS, 341, 823
Lee, J.-W., & Carney, B. W. 2006, AJ, 132, 2171
Markwardt, C. B., & Swank, J. H. 2004, ATel, 255
Marshall, F. E., Swank, J. H., Thomas, B., et al. 1997, IAUC, 6543, 2
Medin, Z., & Cumming, A. 2011, ApJ, 730, 97
Miller, J. M., Cackett, E. M., & Reis, R. C. 2009, ApJL, 707, L77
Negoro, H., Sugizaki, M., Tomida, H., et al. 2010, ATel, 2729
Page, D., & Reddy, S. 2012, arXiv:1201.5602
Remillard, R. 2007, ATel, 1302

Rutledge, R. E., Bildsten, L., Brown, E. F., Pavlov, G. G., & Zavlin, V. E. 2002a, ApJ, 577, 346
Rutledge, R. E., Bildsten, L., Brown, E. F., et al. 2002b, ApJ, 580, 413
Sanchez-Fernandez, C., Chenevez, J., Pavan, L., et al. 2012, ATel, 4304, 1
Sato, K. 1979, PThPh, 62, 957
Schatz, H., Aprahamian, A., Barnard, V., et al. 2001, PhRvL, 86, 3471
Shternin, P. S., Yakovlev, D. G., Haensel, P., & Potekhin, A. Y. 2007, MNRAS, 382, L43
Soria, R., Zampieri, L., Zane, S., & Wu, K. 2011, MNRAS, 410, 1886

Wallace, R. K., & Woosley, S. E. 1981, ApJS, 45, 389
Wijnands, R., Guainazzi, M., van der Klis, M., & Méndez, M. 2002, ApJL, 573, L45
Wijnands, R., Homan, J., Miller, J. M., & Lewin, W. H. G. 2004, ApJL, 606, L61
Wilms, J., Allen, A., & McCray, R. 2000, ApJ, 542, 914
Yamauchi, S. 2010, in The First Year of MAXI: Monitoring Variable X-ray Sources, 27P
Zampieri, L., Turolla, R., Zane, S., & Treves, A. 1995, ApJ, 439, 849